



**HAL**  
open science

# Aqueous phase oligomerization of alpha,beta-unsaturated carbonyls and acids investigated using ion mobility spectrometry coupled to mass spectrometry (IMS-MS)

Pascal Renard, Sabrina Tlili, Sylvain Ravier, Etienne Quivet, Anne Monod

► **To cite this version:**

Pascal Renard, Sabrina Tlili, Sylvain Ravier, Etienne Quivet, Anne Monod. Aqueous phase oligomerization of alpha,beta-unsaturated carbonyls and acids investigated using ion mobility spectrometry coupled to mass spectrometry (IMS-MS). *Atmospheric Environment*, 2016, 130 (SI), pp.153-162. 10.1016/j.atmosenv.2015.10.060 . hal-01436744

**HAL Id: hal-01436744**

**<https://hal.science/hal-01436744>**

Submitted on 2 May 2018

**HAL** is a multi-disciplinary open access archive for the deposit and dissemination of scientific research documents, whether they are published or not. The documents may come from teaching and research institutions in France or abroad, or from public or private research centers.

L'archive ouverte pluridisciplinaire **HAL**, est destinée au dépôt et à la diffusion de documents scientifiques de niveau recherche, publiés ou non, émanant des établissements d'enseignement et de recherche français ou étrangers, des laboratoires publics ou privés.

# Aqueous Phase Oligomerization of $\alpha,\beta$ -unsaturated Carbonyls and Acids Investigated using Ion Mobility Spectrometry Coupled to Mass Spectrometry (IMS-MS)

Pascal Renard, Sabrine Tlili, Sylvain Ravier, Etienne Quivet and Anne Monod\*

Aix Marseille Université, CNRS, LCE FRE 3416, 13331, Marseille, France

\*Corresponding author : telephone: +33 413 55 10 64 /fax : +33 413 55 10 64 and email address: anne.monod@univ-amu.fr

**Key words:** photooxidation, oligomer formation, oligomer characterization, mass spectrometry, traveling wave ion mobility spectrometry.

## Abstract

One of the current essential issues to unravel our ability to forecast future climate change and air quality, implies a better understanding of natural processes leading of secondary organic aerosol (SOA) formation, and in particular the formation and fate of oligomers. The difficulty in characterizing macromolecules is to discern between large oxygenated molecules from series of oligomers containing repeated small monomers of diverse structures.

In the present study, taking advantage from previously established radical vinyl oligomerization of methyl vinylketone (MVK) in the aqueous phase, where relatively simple oligomers containing up to 14 monomers were observed, we have investigated the same reactivity on several other unsaturated water soluble organic compounds (UWSOCs) and on a few mixtures of these precursor compounds. The technique used to characterize the formed oligomers was a traveling wave ion mobility spectrometry coupled to a hybrid quadrupole - time of flight mass spectrometer (IMS-MS) fitted with an electrospray source and ultra-high performance liquid chromatography (UPLC). The technique allows for an additional separation, especially for large ions, containing long carbon chains. We have shown the efficiency of the IMS-mass spectrometry technique to detect oligomers derived from MVK photooxidation in the aqueous phase. The results were then compared to other oligomers, derived from ten other individual biogenic UWSOCs. The technique allowed distinguishing

1 between different oligomers arising from different precursors. It also clearly showed that  
2 compounds bearing a non-conjugated unsaturation did not provide oligomerization. Finally, it  
3 was shown that the IMS-mass spectrometry technique, applied to mixtures of unsaturated  
4 conjugated precursors, exhibited the ability of these precursors to co-oligomerize, i.e.  
5 forming only one complex oligomer system bearing monomers of different structures. The  
6 results are discussed in terms of atmospheric implications for the detection of oligomers in  
7 complex chamber and/or field samples.

## 8 **1. Introduction**

9 Organic aerosols (OA) are well known to play a significant role in many atmospheric  
10 processes resulting in an important impact on climate and human health. Secondary organic  
11 aerosols (SOA) represents almost 80% of OA (Spracklen et al., 2011), and its formation and  
12 growth mechanisms are not well understood. SOA formation is widely attributed to the  
13 oxidation of volatile organic compounds (VOCs) in the dry gas phase, leading to the  
14 formation of less volatile species that subsequently partition into the condensed phase (Claeys  
15 et al., 2004; Donahue et al., 2011; Hallquist et al., 2009; Herrmann et al., 2015; Kanakidou et  
16 al., 2005; Kroll and Seinfeld, 2008). However, under realistic conditions of humidity, the  
17 condensed phase contains liquid water with highly variable mass concentrations as  
18 theoretically predicted (Carlton and Turpin, 2013; Meng et al., 1995; Meng and Seinfeld,  
19 1994; Pilinis et al., 1989) and measured (Nguyen et al., 2014; Tsai and Kuo, 2005).  
20 Therefore, the polar compounds formed during the oxidation of VOCs can readily partition  
21 into the aqueous phase (Blando and Turpin, 2000; Epstein et al., 2013; Ervens et al., 2011a;  
22 Herrmann et al., 2015). Their subsequent chemical reactivity in this phase leads to the  
23 formation of organic acids or higher molecular weight products which can remain at least in  
24 part in the condensed phase when water evaporates. These aqueous processes lead to  
25 additional SOA formation (aqSOA) that can be very different from those in the gas phase,  
26 with likely very different physical and chemical properties (Brégonzio-Rozier et al., 2015;  
27 Carlton et al., 2009; Ervens et al., 2014a; El Haddad et al., 2009; Ortiz-Montalvo et al., 2012;  
28 Renard et al., 2015; Smith et al., 2014).

29 In general,  $\alpha,\beta$ -unsaturated carbonyls  $>C=C-C(=O)-$  and conjugated dienes  $>C=C-C=C<$   
30 are extremely efficient precursors for radical oligomerization (e.g. initiated by  $\cdot OH$  radicals)  
31 in the liquid phase (Clayden et al., 2012; Odian, 2004; Smith and March, 2007), but these  
32 processes have been only scarcely studied under atmospheric conditions (Ervens et al.,  
33 2014a; Ervens et al., 2014b; Kameel et al., 2013a; Liu et al., 2012; Renard et al., 2015, 2013).

1 The authors have shown that the oligomerization proceeds *via* external  $\cdot\text{OH}$ -addition to a  
2 C=C bond, leads to the formation of a hydroxyalkyl radical ( $\text{HO-R}\cdot$ ) that is stabilized by the  
3 resonance effect with the adjacent unsaturation (Figure S1). This  $\text{HOR}\cdot$  radical has a planar  
4 configuration, providing extremely low steric hindrance for further addition (Gilbert et al.,  
5 1994). Thus, in competition with  $\text{O}_2$  addition,  $\text{HOR}\cdot$  radical can easily add to the C=C bond  
6 of another precursor molecule, and quickly propagate the monomer units in this manner, until  
7 the termination step (Figure S1). This termination step is a reaction between two radicals, by  
8 coupling or by disproportionation, thus yielding a series of oligomers, each series being  
9 initialized by a specific radical, depending on the initial  $\cdot\text{OH}$ -attack (Kameel et al., 2013b;  
10 Renard et al., 2013). Renard et al. (2013 and 2015) have studied the effects of the precursor  
11 initial concentrations for methyl vinyl ketone (MVK) under initially aerated solutions, and  
12 they concluded that oligomerization prevails over functionalization for precursor initial  
13 concentrations of 2 mM or higher. In wet aerosol, this concentration range may be reached by  
14 the sum of the unsaturated water soluble organic compounds (UWSOC) (Renard et al., 2013).  
15 However, to our knowledge, the reactivity of mixtures of different atmospherically relevant  
16 UWSOC has never been studied.

17 The ion mobility spectrometry (IMS) is a method to separate and characterize ions based  
18 on their gas-phase transport in electric fields. For roughly 50 years, this technique has been  
19 combined with mass spectrometry (MS) by inserting the IMS separation after ionization e.g.  
20 by electrospray (ESI) and prior to the mass spectrometry step. This combination of an IMS  
21 separation (typically occurring within milliseconds) and MS detection (typically occurring  
22 within microseconds) allows an additional separation step on a MS time-frame, in addition to  
23 liquid chromatography, without compromising the speed of MS detection (Laphorn et al.,  
24 2013; Shvartsburg and Smith, 2008).

25 Although the IMS-MS has been used in different scientific fields (such as structural  
26 polymer chemistry, or biological analyses to fractionate complex mixtures prior to the MS  
27 step), it has only recently been applied for “small molecules” such as those found in the 100-  
28 500 amu (Laphorn et al., 2013). This technique is thus very well suited to analyze  
29 atmospheric oligomers, but, to our knowledge, it has not yet been used in this field.

30 The aim of this work is to investigate aqueous phase oligomerization of several  
31 atmospheric UWSOC through their  $\cdot\text{OH}$ -oxidation using IMS-MS. The efficiency of the  
32 technique is shown on oligomers that were previously described by Renard et al., (2013), i.e.  
33 derived from MVK photooxidation. The results are then compared to other oligomers,

1 derived from other individual biogenic UWSOCs and mixtures of these compounds. The  
2 suitability of the technique for the detection of oligomers in complex chamber and/or field  
3 samples is finally discussed.

## 4 **2. Experimental**

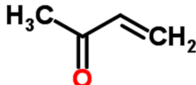
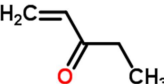
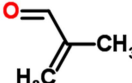
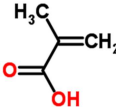
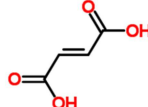
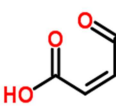
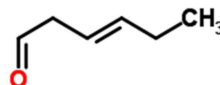
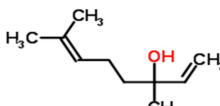
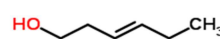
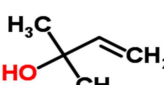
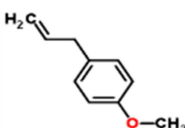
5 A photoreactor was used to simulate the aqueous phase  $\cdot\text{OH}$ -oxidation of UWSOC.  $\cdot\text{OH}$   
6 radicals were generated from  $\text{H}_2\text{O}_2$  photolysis. Liquid samples were collected at specific  
7 reaction times, and analyzed using ultra-performance liquid chromatography (UPLC) coupled  
8 to ion mobility spectrometry and mass spectrometry (IMS-MS). The oligomerization of the  
9 investigated UWSOCs was studied for each individual species, and in mixtures.

### 10 **2.1 Oligomer precursors**

11 Eleven atmospheric relevant UWSOCs (Table 1) were investigated, they were all  
12 purchased from Sigma-Aldrich. The initial reactant concentrations were chosen to scale in the  
13 range of those for which oligomerization was observed previously with MVK (Renard et al.,  
14 2014, 2013) or isoprene (Kameel et al., 2013a). For all experiments, the initial concentration  
15 of  $\text{H}_2\text{O}_2$  was 200 mM. The oligomerization of each individual precursor was examined for an  
16 initial concentration of 10 mM, and the mixtures of precursors were studied starting from a  
17 total UWSOC initial concentration of 10 mM. For the solution mixtures, two control  
18 experiments were performed (in the dark; and under irradiation with no  $\text{H}_2\text{O}_2$ ) and revealed  
19 no oligomer formation. The chosen precursor concentrations correspond to initial carbon  
20 mass concentrations ranging from 480 to 1200  $\text{mgC L}^{-1}$ , depending on the compound (from  
21  $\text{C}_4$  to  $\text{C}_{10}$ ). These concentrations are higher than the total concentrations of WSOC in cloud  
22 and fog droplets, which culminate at approximately 200-300  $\text{mgC L}^{-1}$  (Herckes et al., 2013).  
23 However, they are much lower than the estimated WSOC concentrations in wet aerosols.  
24 Ervens et al. (2011) estimate that these concentrations scale inversely with the volume of the  
25 particles, resulting in typical concentrations of  $\sim\text{M}$  in wet aerosols. Considering that UWSOC  
26 represent 2-20% of WSOC concentrations (Renard et al., 2013), the chosen 10 mM initial  
27 concentration may represent the total concentration of all UWSOCs in wet aerosol.

28 The eleven UWSOC investigated were chosen among a wide range of atmospheric  
29 relevant compounds, such as oxygenated isoprenoids and terpenoids, but also green leaf  
30 volatiles (GLV), Leaf-Wound Oxygenated Compounds (LWOC) and dicarboxylic acids  
31 (Table 1).

32

Compound	Exact mass (amu)	Class <sup>1</sup>	Structure <sup>2</sup>	Maximum degree of Oligomerization <sup>3</sup>
Methyl vinyl ketone (MVK)	70.042	Isop., LWOC	$\alpha,\beta$ -uns. carbonyl 	14
Ethyl vinyl ketone (EVK)	84.058	LWOC	$\alpha,\beta$ -uns. carbonyl 	14
Methacrolein (MACR)	70.042	Isop., LWOC	$\alpha,\beta$ -uns. carbonyl 	12
Methacrylic acid (MA)	86.037	Isop.	$\alpha,\beta$ -uns. acid 	10
Fumaric Acid	116.011	Sec.	$\alpha,\beta$ -uns. acid 	7
Maleic acid	116.011	Sec.	$\alpha,\beta$ -uns. acid 	5
Cis-3-Hexenal	98.073	GLV	$\alpha,\gamma$ -uns. carbonyl 	2
Linalool	154.136	Terp.	non-conjugated diene 	2
Cis-3-Hexen-1-ol	100.089	GLV	uns. alcohol 	/
2-Methyl-3-buten-2-ol (MBO)	86.073	GLV	uns. alcohol 	/
Methyl chavicol	148.088	OBVOC	phenylpropene 	/

1 **Table 1:** List of the eleven studied atmospheric relevant UWSOC. <sup>1</sup> the investigated compounds include  
2 oxygenated isoprenoids (isop.) and terpenoids (terp.), oxygenated biogenic VOC (OBVOC), green leaf volatiles  
3 (GLV), Leaf-Wound Oxygenated Compounds (LWOC) and secondary dicarboxylic acids (sec.). <sup>2</sup> uns. =  
4 unsaturated <sup>3</sup> the maximum degree of oligomerization corresponds to the number of monomer units reached at  
5 the maximum m/z of the most intense oligomer series. Oligomerization is considered to occur for a maximum  
6 degree of oligomerization > 2.  
7

8 MVK, methacrolein (MACR) and methacrylic acid (MA) are key oxidation products of  
9 isoprene, which is the most abundant emitted VOC with a global emission of 500–750 Tg yr<sup>-1</sup>  
10 (Claeys et al., 2004; Guenther et al., 2006). Linalool is a major oxygenated monoterpene  
11 (Geron and Arnsts, 2010). GLV, containing 5 or 6 carbon atoms are initiated by the  
12 lipoxygenase enzymes within plant cells (Jardine et al., 2012). GLV and LWOC emissions

1 can be elevated under different types of stresses, including severe weather, climate change,  
2 mechanical stress, insects, and pathogens (Arneeth et al., 2010; Mentel et al., 2013; Richards-  
3 Henderson et al., 2014). We investigated several GLV that were observed in the atmosphere,  
4 such as cis-3-hexenal, cis-3-hexen-1-ol and 2-methyl-3-buten-2-ol (MBO) (Brilli et al.,  
5 2012; Jardine et al., 2012; Richards-Henderson et al., 2014) and LWOC, such as ethyl vinyl  
6 ketone (EVK) (Jiménez et al., 2009), MACR and MVK (Ruuskanen et al., 2011).

7 Methyl chavicol is a biogenic oxygenated aromatic compound (Bouvier-Brown et al.,  
8 2009a ; Bouvier-Brown et al., 2009b; Pereira et al., 2014), its atmospheric mixing ratios were  
9 reported to be strongly correlated with those of MBO.

10 We also studied three atmospheric unsaturated acids. In addition to methacrylic acid,  
11 we tested two isomers, fumaric and maleic acids. These dicarboxylic acids are secondary  
12 reaction products of both biogenic and anthropogenic precursors. They are highly water  
13 soluble and mostly present in particles, they may be involved with cloud condensation  
14 processes (Sempéré and Kawamura, 2003).

## 15 **2.2 Photoreactor**

16 The photoreactor set-up used was based on the one described in Renard et al. (2013). It is  
17 a 450 cm<sup>3</sup> Pyrex thermostated photoreactor, equipped with a 1000 W xenon arc lamp (LSH  
18 601, Oriel) and a glass filter (AM 0, ASTM 490) to reduce the lamp intensity, in particular in  
19 the infrared range (800 – 1100 nm).

20 All experiments were performed at 25°C. They started with irradiation of aerated UHQ  
21 water (18.2 MΩ cm, Millipore), then H<sub>2</sub>O<sub>2</sub> (50 %, stabilized, Acros) was introduced, and  
22 after 10 min of H<sub>2</sub>O<sub>2</sub> photolysis, the UWSOC was introduced (individually or as a mixture) at  
23 time 0. All experiments were performed in aerated UHQ water, i.e. with initial saturated O<sub>2</sub>  
24 concentrations.

25 For all experiments, the initial ratio  $\frac{[H_2O_2]_0}{[UWSOC]_0} = 20$  was chosen in order to favor  $\cdot OH$   
26 reaction toward UWSOC over its reaction with H<sub>2</sub>O<sub>2</sub> by more than 80 %. Under these  
27 conditions, we estimate that the  $\cdot OH$  concentrations were approximately 10<sup>-14</sup> - 10<sup>-13</sup> M, in  
28 the range of the estimated values for fog droplets to wet aerosol conditions (Arakaki et al.,  
29 2013; Ervens et al., 2014b; Herrmann et al., 2015, 2010).

## 30 **2.3 IMS-mass spectrometry analyses**

31 Aliquots of the solution sampled from the photoreactor were analyzed for oligomers using  
32 an ultra-high performance liquid chromatographic system (UPLC, Waters) coupled to a

1 hybrid quadrupole - time of flight (Q-TOF) mass spectrometer (Synapt-G2 HDMS, Waters)  
2 fitted with an electrospray source (ESI). This instrument incorporates a traveling wave ion  
3 mobility spectrometry (TWIMS). This latter system has been widely described by  
4 (Shvartsburg and Smith, 2008). Briefly, ions are propelled into a chamber containing a buffer  
5 gas and a series of stacked ring electrodes, where a voltage pulse is passed from one to the  
6 next, creating a voltage wave in repeating sequences. The height and the speed of the travel  
7 wave constitute the main internal parameters of this ion mobility cell. Ions with different  
8 collision cross sections (CCS), (i.e., molecular shapes), travel through this ion mobility cell  
9 with different velocities, leading to their mobility-based separation (Laphorn et al., 2013)  
10 which can be quantified using the ion mobility  $K$  given by Equation 1.

$$11 \quad K = \left( \frac{3q}{16N} \right) \sqrt{\left( \frac{2\pi}{\mu k_b T} \right)} \frac{1}{\Omega} \quad \text{Eq. 1}$$

12 Where  $K$  is the ion mobility,  $q$  is the ionic charge [C],  $N$  is the buffer gas density,  $\mu$  is the  
13 reduced mass of the buffer gas and the ion [kg],  $k_b$  is the Boltzman constant [kg m<sup>2</sup> s<sup>-2</sup> K<sup>-1</sup>],  $T$   
14 is the temperature [K], and  $\Omega$  is the collision cross-section (CCS, [Å<sup>2</sup>]).

15 The drift time (DT) of each ion in the cell is inversely proportional to the ion mobility  
16 (Kim et al., 2009; Shvartsburg and Smith, 2008). This technique thus allows for an additional  
17 separation, especially for large ions, with long carbon chains. The instrument thus provides  
18 for each chromatographic peak, 3D spectra: Ion intensity -  $m/z$  – drift time.

19 The chromatographic separations were carried out on an UPLC column (HSS T3 C18, 2.1  
20 × 100 mm – 1.8 μm; Waters) at 40°C. The mobile phases consisted in (A) 0.1 % formic acid  
21 in water (Biosolve, 99 %) and (B) acetonitrile (Biosolve, ULC/MS). The gradient elution was  
22 performed at a flow rate of 600 μL min<sup>-1</sup> using 5 to 95 % of B within 7 min and held at 95 %  
23 of B for 1.5 min. Some contaminant oligomers, e.g., polyethylene glycols (PEG,(Eckers et  
24 al., 2007), appear very often at the end of the run (mostly after 5 min), hence, the detection  
25 peak was systematically performed at retention times ranging from 0 to 4 min.

26 The sample injection volume was 10 μL. The optimum ESI conditions found were as  
27 follows: 0.5 kV capillary voltage, 40 V sample cone voltage, 450°C desolvation temperature,  
28 120°C source temperature, 20 L h<sup>-1</sup> cone gas flow rate and 800 L h<sup>-1</sup> desolvation gas flow  
29 rate. Trap and transfer collision gas flows were set at 2.0 mL min<sup>-1</sup> (0.02 mbar for Ar cell  
30 pressure). Helium cell gas flow was set at 180 mL min<sup>-1</sup>, and IMS gas flow (N<sub>2</sub>) was set at 90  
31 mL min<sup>-1</sup> and 3.0 mbar for IMS cell pressure. Travel wave height and velocity were set at 40  
32 V and 650 m s<sup>-1</sup>, respectively. Data acquisition and mass spectra treatments were provided by



1 the MassLynx software (v.4.1, Waters). Finally, the DriftScope software (v.2.1, Waters) was  
2 used for the treatment of  $m/z$  vs. drift-time maps, and provided 2D IMS-MS spectra. Using  
3 this software, the selected peak detection parameters were the minimum drift time peak width  
4 (0.05 ms), the drift time range (0 to 10.8 ms), the MS resolution (18000) and the minimum  
5 intensity threshold (5000 counts).

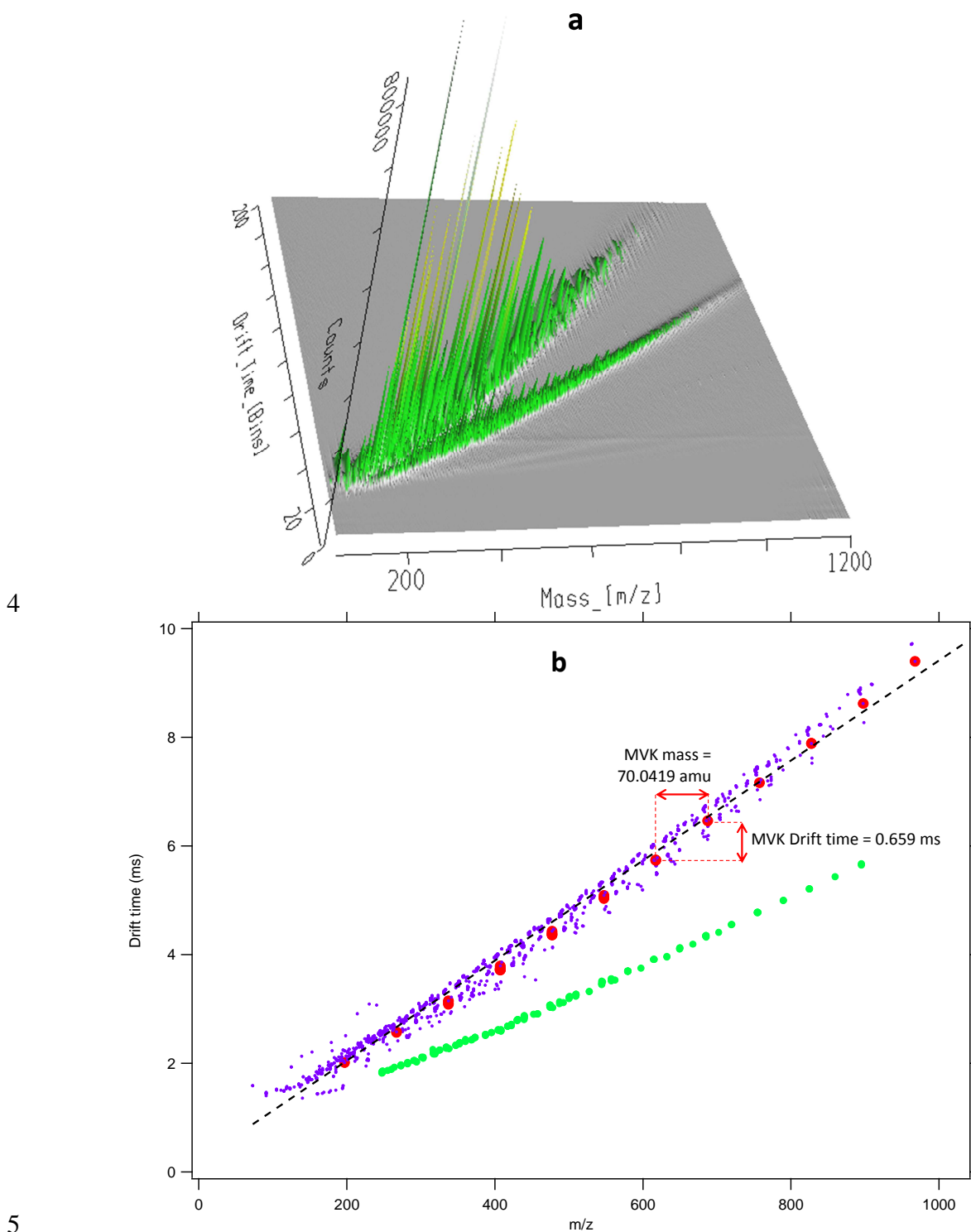
### 6 **3. Results**

7 Using the IMS-MS technique, we studied aqueous phase oligomerization by  $\cdot\text{OH}$ -  
8 oxidation of each individual UWSOC listed in Table 1, starting with MVK, for which  
9 oligomerization processing was previously discussed in detail (Renard et al., 2013). The  
10 results were then compared to other oligomers, derived from the other studied individual  
11 UWSOCs. Finally, the technique was applied to different mixtures of UWSOCs. For each  
12 experiment, the solution was analyzed after 50 min of UWSOC photooxidation, roughly  
13 corresponding to the maximum of oligomer formation for each solution, as observed using  
14 UPLC-ESI-MS.

#### 15 **3.1 Oligomerization of individual precursors evidenced by IMS-mass spectrometry**

16 Figure 1 shows the 3D (Intensity / Drift time /  $m/z$ ) and 2D IMS-MS spectra (in the  
17 positive mode) of the oligomers derived from MVK after 50 min of aqueous phase  $\cdot\text{OH}$ -  
18 oxidation. Generally, each oligomer series is characterized by a recurrent mass  
19 (corresponding to the one of the propagating monomer) and a drift time. In the present  
20 example, the oligomerization is only due to the propagation of one monomer (i.e. MVK),  
21 with a few number of different series, each one corresponding to a different radical initiator  
22 (Renard et al., 2013). The oligomers thus bear highly related structures. As a result, the 2D  
23 IMS-MS spectrum shown in Figure 1 exhibits a linear correlation between the  $m/z$  and the  
24 drift time for all these structure related oligomer series, in good agreement with the  
25 observations by Kim et al., (2009) and Fernandez-Lima et al., (2009) for very different kinds  
26 of molecules (i.e. phosphatidylcholines and crude oils respectively). Its linear regression fit,  
27 derived over four replicate experiments ( $\text{drift time} = 941 (\pm 16) \times 10^{-5} m/z + 0.209 (\pm 0.040)$ )  
28 characterizes the MVK-oligomer system in the positive mode. In Figure 1, the highlighted  
29 red dots label the most intense oligomer series (see the corresponding mass spectrum in  
30 Figure S2). Between two subsequent red dots, one can determine the oligomer series'  
31 characteristic mass (70.0419 amu corresponding to the molecular mass of MVK) and  
32 characteristic drift time (0.659 ms). Figure 1 also shows the double charged ions (green dots),

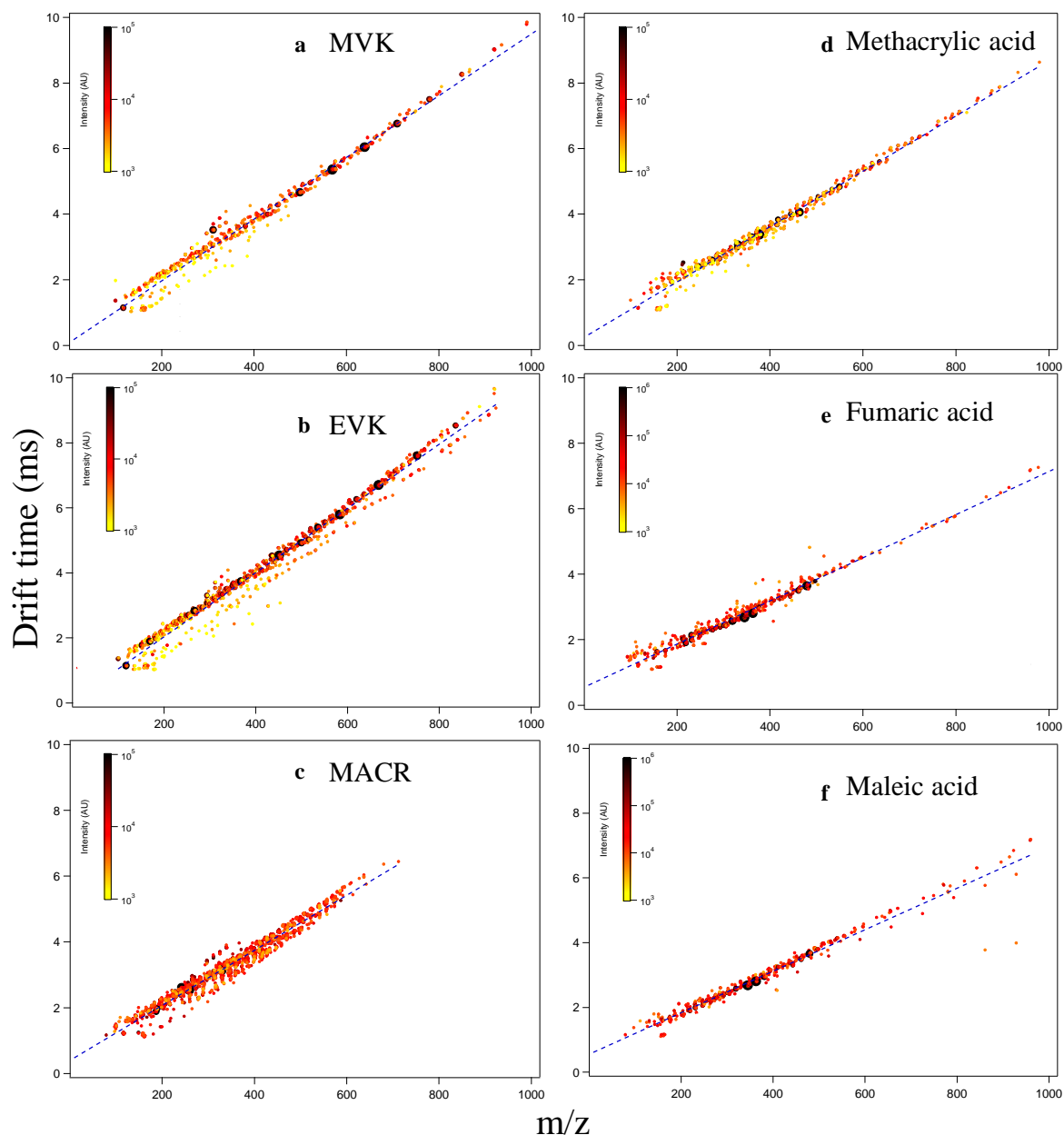
1 which exhibit a significantly lower slope than simply charged ions. In fact, according to Eq.  
2 1, the ion mobility increases (i.e. the drift time decreases) with  $q$ . This explains why double  
3 charged ions show a shorter characteristic drift time than simply charged ions.



5  
6 **Figure 1:** (a) 3D (Intensity / Drift time / m/z) and (b) 2D IMS-MS spectra of MVK after 50 min of  
7 photooxidation in the aqueous phase, in the positive mode. The most intense series is highlighted in red, with its  
8 characteristic MVK mass and MVK drift time. Double charged ions are highlighted in green; they are not  
9 included in the linear regression calculation.

1

2 In the negative mode, the 2D IMS-MS spectrum of the MVK-oligomers (Figure 2a) also  
3 shows a linear correlation between the drift time and  $m/z$  (Table 2), which characterizes the  
4 MVK-oligomer system in the negative mode. The same kind of observations was performed  
5 for all the other individual UWSOCs and mixtures. Thus, we further discuss and compare the  
6 results obtained under exactly the same experimental and analytical conditions using the  
7 negative mode only, as this mode scarcely shows double charged ions.



8  
9 **Figure 2:** 2D IMS-MS spectra (in the negative mode) of different UWSOCs after 50 min of photooxidation in the  
10 aqueous phase. (a) MVK, (b) EVK, (c) MACR, (d) methacrylic acid (e) fumaric acid and (f) maleic acid (in  
11 addition to the color code, dot sizes increase with intensities).

12

1 The 2D IMS-MS spectra obtained for each UWSOC that exhibit oligomerization upon  
2 •OH-oxidation in the aqueous phase, are shown in Figure 2. The maximum degree of  
3 oligomerization (reported in Table 1 and Table 2) (Pearce, 1998) corresponds to the number  
4 of monomer units reached at the maximum m/z of the most intense oligomer series observed.  
5 The precursors are considered to oligomerize under our experimental conditions when the  
6 obtained maximum degree of oligomerization is higher than 2.

7 Table 1 clearly shows that precursor compounds bearing only one unsaturation or two  
8 non-conjugated unsaturations do not provide oligomerization (i.e. maximum degree of  
9 oligomerization < 2). Among these compounds, cis-3-hexenal and linalool undergo only  
10 dimerization: the former is a  $\alpha,\gamma$ -unsaturated carbonyl, and the latter is a non-conjugated  
11 diene. Their dimerization can be the result of radical recombination without propagation.  
12 These results thus confirm the importance of the precursor's chemical structure on the  
13 oligomerization process, and especially the great ability of conjugated unsaturated  
14 compounds to provide oligomer formation under simulated atmospheric conditions.

15 Out of the eleven tested compounds, the six compounds bearing a  $\alpha,\beta$ -unsaturated  
16 conjugation undergo oligomerization (Table 1). Figure 2 shows that, in the same manner as  
17 for MVK, for all these compounds, the m/z and the ion mobility are strongly correlated.  
18 However, important differences are observed from one precursor to the other on the  
19 maximum degree of oligomerization, on the number of oligomer series, or on the drift. MVK  
20 and EVK show the highest maximum degree of oligomerization (14). This result is consistent  
21 with the fact that these two compounds have very similar chemical structures, and thus they  
22 oligomerize in the same way. This is further confirmed by the fact that the linear correlations  
23 between the drift and m/z of their oligomers exhibit the same slope for both precursors,  
24 within the experimental uncertainties (Table 2).

25 The IMS-MS technique also evidences substantial differences between the oligomers  
26 arising from MVK and MACR (Figures 2a and 2c) although these two precursors are  
27 isomers. The lower DT-m/z slope obtained for MACR-oligomers (Table 2) indicates that they  
28 oligomerize in different ways. Compared to MVK-oligomers, MACR-oligomers also show a  
29 significantly more clustered shape of the 2D IMS-MS spectra (Figure 2), with more scattered  
30 data points, a lower correlation coefficient and a lower maximum degree of oligomerization  
31 (Table 2). These differences can be due to a more complex oligomer system (Kim et al.,  
32 2009) with MACR precursor, as discussed further hereafter.

Methacrylic acid (Figure 2d) is one of the reaction products of MACR photooxidation in the aqueous phase (Liu et al., 2009). Its oligomers exhibit statistically the same slope as those arising from MACR (Table 2). These observations can be the result of common oligomer series arising from both MACR and methacrylic acid, and thus can explain in part the more complex oligomer system observed from MACR than from MVK.

Fumaric and maleic acids are conformers (Table 1), the former one being produced from the natural photolysis of the latter one under atmospheric conditions (Fu et al., 2013). Although the IMS-MS technique is commonly used to distinguish between oligomers arising from isomers (Li et al., 2012), maleic and fumaric acids exhibit oligomers with similar trends in the 2D IMS-MS spectra (Figures 2e and 2f) and statistically the same slope (Table 2). However, the slopes obtained are significantly lower than those observed from the oligomers arising from the other precursors.

Compounds	Equation of drift time = $f(m/z)$ ( $\pm$ Standard deviation)	Maximum Degree of Oligomerization
Methyl vinyl ketone (MVK)	$DT = 947 (\pm 6) \times 10^{-5} m/z + 0.051 (\pm 0.017)$	14
Ethyl vinyl ketone (EVK)	$DT = 968 (\pm 27) \times 10^{-5} m/z + 0.855 (\pm 0.040)$	14
Methacrolein (MACR)	$DT = 879 (\pm 59) \times 10^{-5} m/z + 0.217 (\pm 0.254)$	12
Methacrylic acid	$DT = 844 (\pm 15) \times 10^{-5} m/z + 0.226 (\pm 0.056)$	10
Fumaric acid	$DT = 687 (\pm 37) \times 10^{-5} m/z + 0.426 (\pm 0.167)$	7
Maleic acid	$DT = 668 (\pm 37) \times 10^{-5} m/z + 0.445 (\pm 0.151)$	5
Mixtures	Equation of drift time = $f(m/z)$ ( $\pm$ Standard deviation)	Maximum degree of Oligomerization
MVK + MACR	$DT = 915 (\pm 16) \times 10^{-5} m/z + 0.098 (\pm 0.024)$	8
Fumaric + Maleic acids	$DT = 671 (\pm 12) \times 10^{-5} m/z + 0.488 (\pm 0.121)$	4
Fumaric + Maleic + methacrylic acids	$DT = 734 (\pm 13) \times 10^{-5} m/z + 0.430 (\pm 0.106)$	5 <sup>a</sup>
MVK + MACR + EVK + Fumaric + Maleic + methacrylic acids	$DT = 891 (\pm 15) \times 10^{-5} m/z + 0.165 (\pm 0.041)$	8 <sup>a</sup>

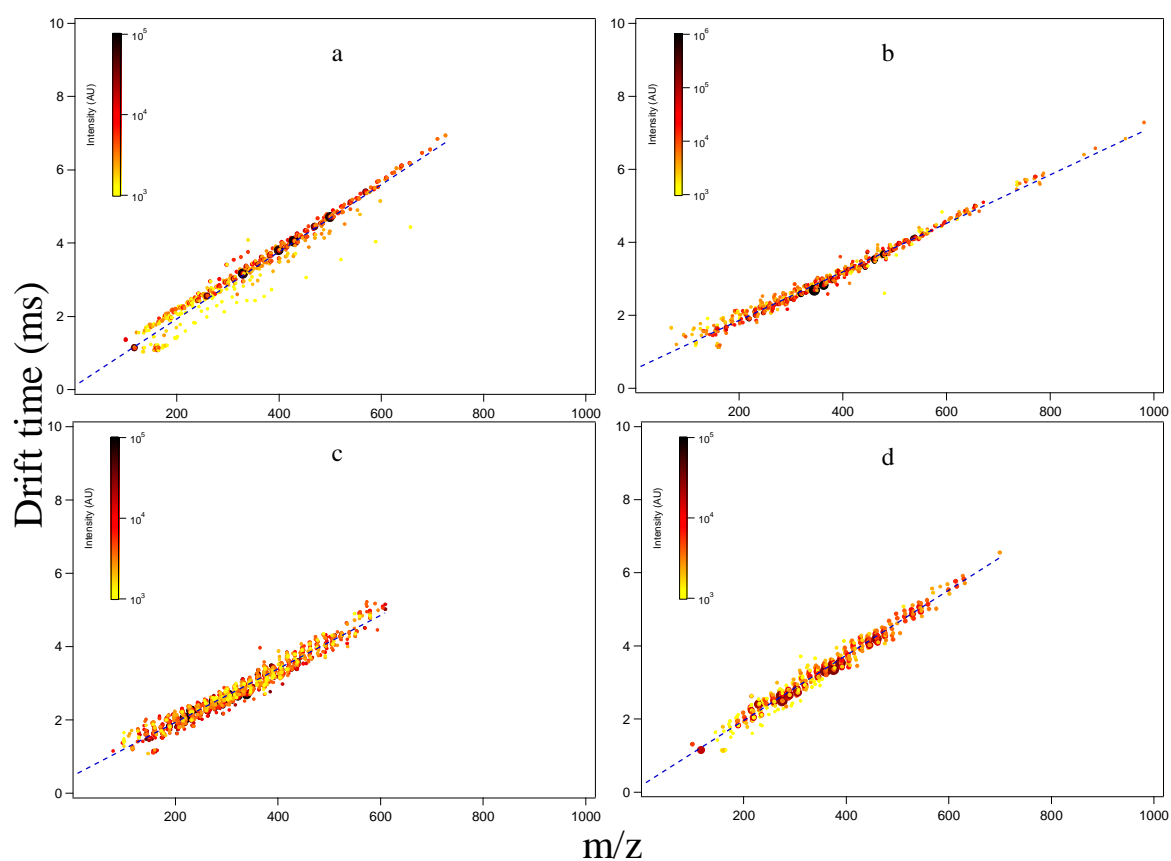
**Table 2 :** Linear regression of the drift time (DT) as a function of  $m/z$ ; and maximum degree of oligomerization obtained from the investigated oligomer precursors: six individual  $\alpha$ - $\beta$  unsaturated UWSOCs and four mixtures, by means of IMS-MS in the negative mode. The statistical data were derived over 1 to 4 replicate experiments. <sup>a</sup> for complex mixtures, the maximum degree of co-oligomerization corresponds to the maximum  $m/z$  reached by the most intense series, divided by the average molar mass of the mixture.

### 3.2 Co-oligomerization of precursor mixtures evidenced by IMS-mass spectrometry

In order to examine more complex mixtures, i.e. closer to atmospheric conditions, we investigate in this section IMS-MS analyses of different mixtures of the six compounds bearing a  $\alpha$ , $\beta$ -unsaturated conjugation that individually undergo oligomerization, as shown in the previous section. The aim is to observe oligomerization or co-oligomerization of mixtures containing the same initial total concentration as that used for each individual precursor (10

1 mM). Due to the different oligomer properties evidenced for the individual precursors, the  
2 IMS-MS is a valuable technique to examine if these precursors can undergo co-  
3 oligomerization when mixed together. Co-oligomerization is the formation of an oligomer  
4 derived from more than one species of monomer. Such co-oligomers, in which there is an  
5 irregular distribution of different monomers, mainly follows the Bernoulli Law (O dian,  
6 2004). In this case, co-oligomers can theoretically also be statistically characterized by the  
7 slope of the 2D IMS-MS linear regression fit formed by the detected peaks.

8 Figure 3 shows that this phenomenon is observed for the four different mixtures of  
9 precursors investigated. Such mixtures show extremely complex mass spectra, from which  
10 interpretation is arduous if not impossible (see for example Figure S3), whereas IMS-MS  
11 spectra exhibit a linear correlation between the  $m/z$  and the drift time which proves  
12 indubitably co-oligomerization.



13  
14 **Figure 3:** 2D IMS-MS of four different mixtures of  $\alpha$ - $\beta$  unsaturated carbonyls and acids after 50 min of  
15 photooxidation in the aqueous phase, in the negative mode, with the equations of drift time (standard deviations  
16 are in table 2) arising from aqueous phase photooxidation of (a) MVK + MACR (5 mM each), (b) fumaric +  
17 maleic acids (5 mM each), (c) fumaric + maleic + methacrylic acids (3.33 mM each), (d) MVK + MACR +  
18 EVK + Fumaric + Maleic + methacrylic acids (1.67 mM each).  
19

1 For the mixture of MVK + MACR (5 mM each), the 2D IMS-MS spectrum (Figure 3a)  
2 shows a linear regression fit with an intermediate slope value between those arising from  
3 MVK and MACR individually (Table 2).

4 This result confirms that we do not obtain two different oligomer systems, but rather one  
5 co-oligomerization system. The maximum degree of co-oligomerization is smaller than those  
6 arising from each individual precursors (Table 2). However, the number of series is likely  
7 higher (Figure 3a), certainly due to the enhanced complexity of the system.

8 For the mixture of maleic and fumaric acids (5mM each), the 2D IMS-MS spectrum  
9 (Figure 3b) shows statistically the same slope as those obtained from each individual acid  
10 (Table 2). It is thus not possible to determine if any co-oligomerization is occurring in this  
11 case.

12 For the mixture of maleic, fumaric and methacrylic acids (3.33 mM each) (Figure 3c), we  
13 observe one intermediate slope between the value obtained for the previous mixture (Figure  
14 3b) and that obtained for methacrylic acid alone (Table 2). The system becomes more  
15 complex, with likely more oligomer series as denoted by the more clustered shape of the 2D  
16 IMS-MS spectra and a lower maximum degree of co-oligomerization (Table 2). Note that, in  
17 this case where co-oligomers contain various monomers of various molecular masses, the  
18 maximum degree of co-oligomerization is only an estimated value as it corresponds to the  
19 maximum m/z reached by the most intense series observed, divided by the average molecular  
20 mass of the initial mixture.

21 For the final mixture of the six  $\alpha,\beta$ -unsaturated conjugated compounds (1,67 mM each),  
22 the 2D IMS-MS spectrum also shows a highly correlated linear plot (Figure 3d) with an  
23 intermediate slope between the six individual compounds (Table 2), with a likely more  
24 complex oligomer system, and more oligomer series.

#### 25 **4. Conclusions and atmospheric implications**

26 One of the current essential issues to unravel our ability to forecast future climate change  
27 and air quality, implies a better understanding of natural processes leading to SOA formation,  
28 and in particular the formation and fate of macromolecules. The presence of macromolecules  
29 in the atmosphere has previously been monitored by ultrahigh resolution mass spectrometry  
30 techniques which have revealed the presence of organic molecules containing up to 35 carbon  
31 atoms (C<sub>35</sub>) in aerosol (Kourtchev et al., 2014; LeClair et al., 2012; Mazzoleni et al., 2012;  
32 Rincón et al., 2012), in fog (Mazzoleni et al., 2010) and in rain (Mead et al., 2015, 2013).  
33 Evidence that condensed-phase reactions contribute to SOA has been obtained from

1 laboratory and smog chamber studies (Hallquist et al., 2009; Hall and Johnston, 2012;  
2 Herrmann et al., 2015; Zhao et al., 2012). From these studies, it seems that a substantial  
3 amount of SOA is composed of oligomers. The latter are small polymers containing less than  
4 30 monomers. The difficulty in characterizing such molecules is to discern between large  
5 oxygenated molecules from series of oligomers containing repeated small monomers of  
6 diverse structures (Nozière et al., 2015).

7 In the present study, taking advantage from previously established radical vinyl  
8 oligomerization of MVK in the aqueous phase (Renard et al., 2013) where relatively simple  
9 oligomers containing up to 14 monomers were observed, we have investigated the same  
10 reactivity on several other UWSOCs and on a few mixtures of these precursor compounds.  
11 The technique used to characterize the formed oligomers was a traveling wave ion mobility  
12 spectrometry coupled to a hybrid quadrupole - time of flight mass spectrometer (IMS-MS)  
13 fitted with an electrospray source and UPLC. The technique allows for an additional  
14 separation, especially for large ions, containing long carbon chains. The technique is  
15 currently widely used in polymer chemistry, or biological analyses, it has only recently been  
16 applied for “small molecules” such as those found in the  $m/z$  100-500 range. This technique  
17 is thus very well suited to analyze atmospheric oligomers, but, to our knowledge, it has not  
18 yet been used in this field.

19 We have shown in this study the efficiency of the IMS-mass spectrometry technique on  
20 oligomers derived from MVK photooxidation in the aqueous phase. The results were then  
21 compared to other oligomers, derived from ten other individual biogenic UWSOCs:  
22 methacrolein, ethyl vinylketone, methacrylic acid, fumaric and maleic acids, cis-3-hexenal,  
23 linalool, cis-3-hexen-1-ol, 2-methyl-3-buten-2-ol and methyl chavicol. The technique allowed  
24 distinguishing between different oligomers arising from different precursors. It also clearly  
25 showed that compounds bearing a non-conjugated unsaturation did not provide  
26 oligomerization. Finally, it was shown that the IMS-mass spectrometry technique, applied to  
27 mixtures of unsaturated conjugated precursors, exhibited the ability of these precursors to co-  
28 oligomerize, i.e. forming only one complex oligomer system bearing monomers of different  
29 structures.

30 These observations demonstrate the effectiveness of using IMS-mass spectrometry in the  
31 study of atmospheric oligomer systems. IMS-mass spectrometry has significant advantages  
32 for the analysis of very complex mixtures. It provides rapid identification of complex  
33 oligomer systems, when mass spectra are extremely difficult to interpret. In this way, the  
34 technique can be regarded as an excellent complement to the ultrahigh resolution mass



1 spectrometry techniques when long chain complex oligomer series are suspected to be  
2 formed, as previously demonstrated on crude oil analyses by Fernandez-Lima et al. (2009).  
3 Thus, there should be a growing interest in the use of IMS-mass spectrometry in atmospheric  
4 studies to assist in the deconvolution of complex chamber and field samples.

5

6 **Acknowledgements.** We thank the National Research Agency ANR (project CUMULUS  
7 ANR-2010-BLAN-617-01), AXA insurances. The authors thank Jean-Louis Clément (Aix  
8 Marseille Université CNRS, ICR UMR7273, 13397, Marseille, France) for valuable  
9 discussions on the reactivity of the different various compounds studied.

## 10 **References**

- 11 Arakaki, T., Anastasio, C., Kuroki, Y., Nakajima, H., Okada, K., Kotani, Y., Handa, D.,  
12 Azechi, S., Kimura, T., Tshako, A., Miyagi, Y., 2013. A General Scavenging Rate  
13 Constant for Reaction of Hydroxyl Radical with Organic Carbon in Atmospheric  
14 Waters. *Environ. Sci. Technol.* 47, 8196-8203. doi:10.1021/es401927b
- 15 Arneeth, A., Harrison, S.P., Zaehle, S., Tsigaridis, K., Menon, S., Bartlein, P.J., Feichter, J.,  
16 Korhola, A., Kulmala, M., O'Donnell, D., Schurgers, G., Sorvari, S., Vesala, T.,  
17 2010. Terrestrial biogeochemical feedbacks in the climate system. *Nat. Geosci* 3,  
18 525–532. doi:10.1038/ngeo905
- 19 Blando, J.D., Turpin, B.J., 2000. Secondary organic aerosol formation in cloud and fog  
20 droplets: a literature evaluation of plausibility. *Atmos. Environ.* 34, 1623–1632.  
21 doi:10.1016/S1352-2310(99)00392-1
- 22 Bouvier-Brown, N.C., Goldstein, A.H., Worton, D.R., Matross, D.M., Gilman, J.B., Kuster,  
23 W.C., Welsh-Bon, D., Warneke, C., de Gouw, J.A., Cahill, T.M., others, 2009a.  
24 Methyl chavicol: characterization of its biogenic emission rate, abundance, and  
25 oxidation products in the atmosphere. *Atmospheric Chem. Phys.* 9, 2061–2074.
- 26 Bouvier-Brown, N.C., Holzinger, R., Palitzsch, K., Goldstein, A.H., 2009b. Large emissions  
27 of sesquiterpenes and methyl chavicol quantified from branch enclosure  
28 measurements. *Atmos. Environ.* 43, 389–401. doi:10.1016/j.atmosenv.2008.08.039
- 29 Brégonzio-Rozier, L., Siekmann, F., Giorio, C., Pangui, E., Morales, S.B., Temime-Roussel,  
30 B., Gratien, A., Michoud, V., Ravier, S., Cazaunau, M., Tapparo, A., Monod, A.,  
31 Doussin, J.-F., 2015. Gaseous products and secondary organic aerosol formation  
32 during long term oxidation of isoprene and methacrolein. *Atmos Chem Phys* 15,  
33 2953–2968. doi:10.5194/acp-15-2953-2015

- 1 Brill, F., Hörtnagl, L., Bamberger, I., Schnitzhofer, R., Ruuskanen, T.M., Hansel, A., Loreto,  
2 F., Wohlfahrt, G., 2012. Qualitative and Quantitative Characterization of Volatile  
3 Organic Compound Emissions from Cut Grass. *Environ. Sci. Technol.* 46, 3859–  
4 3865. doi:10.1021/es204025y
- 5 Carlton, A.G., Turpin, B.J., 2013. Particle partitioning potential of organic compounds is  
6 highest in the Eastern US and driven by anthropogenic water. *Atmospheric Chem.*  
7 *Phys.* 13, 10203–10214. doi:10.5194/acp-13-10203-2013
- 8 Carlton, A.G., Wiedinmyer, C., Kroll, J.H., 2009. A review of Secondary Organic Aerosol  
9 (SOA) formation from isoprene. *Atmospheric Chem. Phys.* 9, 4987–5005.
- 10 Claeys, M., Wang, W., Ion, A.C., Kourtchev, I., Gelencsér, A., Maenhaut, W., 2004.  
11 Formation of secondary organic aerosols from isoprene and its gas-phase oxidation  
12 products through reaction with hydrogen peroxide. *Atmos. Environ.* 38, 4093–4098.  
13 doi:10.1016/j.atmosenv.2004.06.001
- 14 Clayden, J., Greeves, N., Warren, S., 2012. *Organic Chemistry*. Oxford University Press,  
15 Oxford.
- 16 Donahue, N.M., Epstein, S.A., Pandis, S.N., Robinson, A.L., 2011. A two-dimensional  
17 volatility basis set: 1. organic-aerosol mixing thermodynamics. *Atmospheric Chem.*  
18 *Phys.* 11, 3303–3318. doi:10.5194/acp-11-3303-2011
- 19 Eckers, C., Laures, A.M.-F., Giles, K., Major, H., Pringle, S., 2007. Evaluating the utility of  
20 ion mobility separation in combination with high-pressure liquid  
21 chromatography/mass spectrometry to facilitate detection of trace impurities in  
22 formulated drug products. *Rapid Commun. Mass Spectrom.* 21, 1255–1263.  
23 doi:10.1002/rcm.2938
- 24 Epstein, S.A., Tapavicza, E., Furche, F., Nizkorodov, S.A., 2013. Direct photolysis of  
25 carbonyl compounds dissolved in cloud and fog~droplets. *Atmospheric Chem. Phys.*  
26 13, 9461–9477. doi:10.5194/acp-13-9461-2013
- 27 Ervens, B., Renard, P., Ravier, S., Clément, J.-L., Monod, A., 2014a. Aqueous phase  
28 oligomerization of methyl vinyl ketone through photooxidation - Part 2: Development  
29 of the chemical mechanism and atmospheric implications. *Atmospheric Chem. Phys.*  
30 *Discuss.* 14, 21565–21609. doi:10.5194/acpd-14-21565-2014
- 31 Ervens, B., Sorooshian, A., Lim, Y.B., Turpin, B.J., 2014b. Key parameters controlling OH-  
32 initiated formation of secondary organic aerosol in the aqueous phase (aqSOA). *J.*  
33 *Geophys. Res. Atmospheres* 119, 3997–4016. doi:10.1002/2013JD021021

- 1 Ervens, B., Turpin, B.J., Weber, R.J., 2011a. Secondary organic aerosol formation in cloud  
2 droplets and aqueous particles (aqSOA): a review of laboratory, field and model  
3 studies. *Atmospheric Chem. Phys.* 11, 11069–11102. doi:10.5194/acp-11-11069-2011
- 4 Ervens, B., Turpin, B.J., Weber, R.J., 2011b. Secondary organic aerosol formation in cloud  
5 droplets and aqueous particles (aqSOA): a review of laboratory, field and model  
6 studies. *Atmospheric Chem. Phys.* 11, 11069–11102. doi:10.5194/acp-11-11069-2011
- 7 Fernandez-Lima F, Fernandez-Lima A., Becker C., McKenna A.M., Rodgers R.P., Marshall  
8 A.G., Russell D.H.. Petroleum Crude Oil Characterization by IMS-MS and FTICR  
9 MS. *Anal. Chem.* 2009, 81, 9941–9947
- 10 Fu, P.Q., Kawamura, K., Chen, J., Charrière, B., Sempéré, R., 2013. Organic molecular  
11 composition of marine aerosols over the Arctic Ocean in summer: contributions of  
12 primary emission and secondary aerosol formation. *Biogeosciences* 10, 653–667.  
13 doi:10.5194/bg-10-653-2013
- 14 Geron, C.D., Arnts, R.R., 2010. Seasonal monoterpene and sesquiterpene emissions from  
15 *Pinus taeda* and *Pinus virginiana*. *Atmos. Environ.* 44, 4240–4251.  
16 doi:10.1016/j.atmosenv.2010.06.054
- 17 Gilbert, B.C., Smith, J.R.L., Milne, E.C., Whitwood, A.C., Taylor, P., 1994. Kinetic and  
18 structural EPR studies of radical polymerization. Monomer, dimer, trimer and mid-  
19 chain radicals formed via the initiation of polymerization of acrylic acid and related  
20 compounds with electrophilic radicals ( $\cdot\text{OH}$ ,  $\text{SO}_4^{\cdot-}$  and  $\text{Cl}_2^{\cdot-}$ ). *J. Chem. Soc. Perkin*  
21 *Trans.* 2 1759–1769. doi:10.1039/P29940001759
- 22 Guenther, A., Karl, T., Harley, P., Wiedinmyer, C., Palmer, P.I., Geron, C., others, 2006.  
23 Estimates of global terrestrial isoprene emissions using MEGAN (Model of Emissions  
24 of Gases and Aerosols from Nature). *Atmospheric Chem. Phys.* 6, 3181–3210.
- 25 El Haddad, I.E., Liu, Y., Nieto-Gligorovski, L., Michaud, V., Temime-Roussel, B., Quivet,  
26 E., Marchand, N., Sellegri, K., Monod, A., 2009. In-cloud processes of methacrolein  
27 under simulated conditions–Part 2: Formation of secondary organic aerosol.  
28 *Atmospheric Chem. Phys.* 9, 5107–5117.
- 29 Hallquist, M., Wenger, J., Baltensperger, U., Rudich, Y., Simpson, D., Claeys, M., Dommen,  
30 J., Donahue, N.M., George, C., Goldstein, A.H., Hamilton, J.V., Herrmann, H.,  
31 Hoffmann, T., Iinuma, Y., Jang, M., Jenkin, M.E., Jimenez, J.L., Kiendler-Scharr, A.,  
32 Maenhaut, W., McFiggans, G.B., Mentel, T.F., Monod, A., Prevot, A.S.H., Seinfeld,  
33 J.H., Surratt, J.D., Szmigielski, R., wild, 2009. The formation, properties and impact

1 of secondary organic aerosol: current and emerging issues. *Atmospheric Chem. Phys.*  
2 9, 5155–5236. doi:10.5194/acp-9-5155-2009

3 Hall, W.A., Johnston, M.V., 2012. Oligomer Formation Pathways in Secondary Organic  
4 Aerosol from MS and MS/MS Measurements with High Mass Accuracy and  
5 Resolving Power. *J. Am. Soc. Mass Spectrom.* 23, 1097–1108. doi:10.1007/s13361-  
6 012-0362-6

7 Herckes, P., Valsaraj, K.T., Collett, J.L., 2013. A review of observations of organic matter in  
8 fogs and clouds: Origin, processing and fate. *Atmospheric Res.* 132-133, 434–449.  
9 doi:10.1016/j.atmosres.2013.06.005

10 Herrmann, H., Hoffmann, D., Schaefer, T., Brüner, P., Tilgner, A., 2010. Tropospheric  
11 Aqueous-Phase Free-Radical Chemistry: Radical Sources, Spectra, Reaction Kinetics  
12 and Prediction Tools. *ChemPhysChem* 11, 3796–3822. doi:10.1002/cphc.201000533

13 Herrmann, H., Schaefer, T., Tilgner, A., Styler, S.A., Weller, C., Teich, M., Otto, T., 2015.  
14 Tropospheric Aqueous-Phase Chemistry: Kinetics, Mechanisms, and Its Coupling to a  
15 Changing Gas Phase. *Chem. Rev.* 115, 4259–4334. doi:10.1021/cr500447k

16 Jardine, K., Barron-Gafford, G.A., Norman, J.P., Abrell, L., Monson, R.K., Meyers, K.T.,  
17 Pavao-Zuckerman, M., Dontsova, K., Kleist, E., Werner, C., Huxman, T.E., 2012.  
18 Green leaf volatiles and oxygenated metabolite emission bursts from mesquite  
19 branches following light–dark transitions. *Photosynth. Res.* 113, 321–333.  
20 doi:10.1007/s11120-012-9746-5

21 Jiménez, E., Lanza, B., Antiñolo, M., Albaladejo, J., 2009. Photooxidation of Leaf-Wound  
22 Oxygenated Compounds, 1-Penten-3-ol, ( *Z* )-3-Hexen-1-ol, and 1-Penten-3-one,  
23 Initiated by OH Radicals and Sunlight. *Environ. Sci. Technol.* 43, 1831–1837.  
24 doi:10.1021/es8027814

25 Kameel, F.R., Hoffmann, M.R., Colussi, A.J., 2013a. OH Radical-Initiated Chemistry of  
26 Isoprene in Aqueous Media. Atmospheric Implications. *J. Phys. Chem. A* 117, 5117–  
27 5123. doi:10.1021/jp4026267

28 Kameel, F.R., Hoffmann, M.R., Colussi, A.J., 2013b. OH Radical-Initiated Chemistry of  
29 Isoprene in Aqueous Media. Atmospheric Implications. *J. Phys. Chem. A* 117, 5117–  
30 5123. doi:10.1021/jp4026267

31 Kanakidou, M., Seinfeld, J.H., Pandis, S.N., Barnes, I., Dentener, F.J., Facchini, M.C.,  
32 Dingenen, R.V., Ervens, B., Nenes, A., Nielsen, C.J., others, 2005. Organic aerosol  
33 and global climate modelling: a review. *Atmospheric Chem. Phys.* 5, 1053–1123.

- 1 Kim, H.I., Kim, H., Pang, E.S., Ryu, E.K., Beegle, L.W., Loo, J.A., Goddard, W.A., Kanik,  
2 I., 2009. Structural Characterization of Unsaturated Phosphatidylcholines Using  
3 Traveling Wave Ion Mobility Spectrometry. *Anal. Chem.* 81, 8289–8297.  
4 doi:10.1021/ac900672a
- 5 Kourtchev, I., Fuller, S.J., Giorio, C., Healy, R.M., Wilson, E., O'Connor, I., Wenger, J.C.,  
6 McLeod, M., Aalto, J., Ruuskanen, T.M., Maenhaut, W., Jones, R., Venables, D.S.,  
7 Sodeau, J.R., Kulmala, M., Kalberer, M., 2014. Molecular composition of biogenic  
8 secondary organic aerosols using ultrahigh-resolution mass spectrometry: comparing  
9 laboratory and field studies. *Atmos Chem Phys* 14, 2155–2167. doi:10.5194/acp-14-  
10 2155-2014
- 11 Kroll, J.H., Seinfeld, J.H., 2008. Chemistry of secondary organic aerosol: Formation and  
12 evolution of low-volatility organics in the atmosphere. *Atmos. Environ.* 42, 3593–  
13 3624. doi:10.1016/j.atmosenv.2008.01.003
- 14 Laphorn, C., Pullen, F., Chowdhry, B.Z., 2013a. Ion mobility spectrometry-mass  
15 spectrometry (IMS-MS) of small molecules: Separating and assigning structures to  
16 ions. *Mass Spectrom. Rev.* 32, 43–71. doi:10.1002/mas.21349
- 17 LeClair, J.P., Collett, J.L., Mazzoleni, L.R., 2012. Fragmentation Analysis of Water-Soluble  
18 Atmospheric Organic Matter Using Ultrahigh-Resolution FT-ICR Mass Spectrometry.  
19 *Environ. Sci. Technol.* 46, 4312–4322. doi:10.1021/es203509b
- 20 Li, H., Giles, K., Bendiak, B., Kaplan, K., Siems, W.F., Hill, H.H., 2012. Resolving  
21 Structural Isomers of Monosaccharide Methyl Glycosides Using Drift Tube and  
22 Traveling Wave Ion Mobility Mass Spectrometry. *Anal. Chem.* 84, 3231–3239.  
23 doi:10.1021/ac203116a
- 24 Liu, Y., El Haddad, I.E., Scarfogliero, M., Nieto-Gligorovski, L., Temime-Roussel, B.,  
25 Quivet, E., Marchand, N., Picquet-Varrault, B., Monod, A., 2009. In-cloud processes  
26 of methacrolein under simulated conditions–Part 1: Aqueous phase photooxidation.  
27 *Atmospheric Chem. Phys.* 9, 5093–5105.
- 28 Liu, Y., Siekmann, F., Renard, P., El Zein, A., Salque, G., El Haddad, I., Temime-Roussel,  
29 B., Voisin, D., Thissen, R., Monod, A., 2012. Oligomer and SOA formation through  
30 aqueous phase photooxidation of methacrolein and methyl vinyl ketone. *Atmos.*  
31 *Environ.* 49, 123–129. doi:10.1016/j.atmosenv.2011.12.012
- 32 Mazzoleni, L.R., Ehrmann, B.M., Shen, X., Marshall, A.G., Collett, J.L., 2010. Water-  
33 Soluble Atmospheric Organic Matter in Fog: Exact Masses and Chemical Formula

1 Identification by Ultrahigh-Resolution Fourier Transform Ion Cyclotron Resonance  
2 Mass Spectrometry. *Environ. Sci. Technol.* 44, 3690–3697. doi:10.1021/es903409k

3 Mazzoleni, L.R., Saranjampour, P., Dalbec, M.M., Samburova, V., Hallar, A.G., Zielinska,  
4 B., Lowenthal, D.H., Kohl, S., 2012. Identification of water-soluble organic carbon in  
5 non-urban aerosols using ultrahigh-resolution FT-ICR mass spectrometry: organic  
6 anions. *Environ. Chem.* 9, 285. doi:10.1071/EN11167

7 Mead, R.N., Felix, J.D., Avery, G.B., Kieber, R.J., Willey, J.D., Podgorski, D.C., 2015.  
8 Characterization of CHOS compounds in rainwater from continental and coastal  
9 storms by ultrahigh resolution mass spectrometry. *Atmos. Environ.* 105, 162–168.  
10 doi:10.1016/j.atmosenv.2015.01.057

11 Mead, R.N., Mullaugh, K.M., Brooks Avery, G., Kieber, R.J., Willey, J.D., Podgorski, D.C.,  
12 2013. Insights into dissolved organic matter complexity in rainwater from continental  
13 and coastal storms by ultrahigh resolution Fourier transform ion cyclotron resonance  
14 mass spectrometry. *Atmospheric Chem. Phys.* 13, 4829–4838. doi:10.5194/acp-13-  
15 4829-2013

16 Meng, Z., Seinfeld, J.H., 1994. On the Source of the Submicrometer Droplet Mode of Urban  
17 and Regional Aerosols. *Aerosol Sci. Technol.* 20, 253–265.  
18 doi:10.1080/02786829408959681

19 Meng, Z., Seinfeld, J.H., Saxena, P., Kim, Y.P., 1995. Contribution of Water to Particulate  
20 Mass in the South Coast Air Basin. *Aerosol Sci. Technol.* 22, 111–123.  
21 doi:10.1080/02786829408959731

22 Mentel, T.F., Kleist, E., Andres, S., Dal Maso, M., Hohaus, T., Kiendler-Scharr, A., Rudich,  
23 Y., Springer, M., Tillmann, R., Uerlings, R., Wahner, A., Wildt, J., 2013. Secondary  
24 aerosol formation from stress-induced biogenic emissions and possible climate  
25 feedbacks. *Atmospheric Chem. Phys.* 13, 8755–8770. doi:10.5194/acp-13-8755-2013

26 Nguyen, T.K.V., Petters, M.D., Suda, S.R., Carlton, A.G., 2014. Trends in particle phase  
27 liquid water during the Southern Oxidant and Aerosol Study. *Atmospheric Chem.*  
28 *Phys.* 4, 10911–10930.

29 Nozière, B., Kalberer, M., Claeys, M., Allan, J., D’Anna, B., Decesari, S., Finessi, E.,  
30 Glasius, M., Grgić, I., Hamilton, J.F., Hoffmann, T., Iinuma, Y., Jaoui, M., Kahnt, A.,  
31 Kampf, C.J., Kourtschev, I., Maenhaut, W., Marsden, N., Saarikoski, S., Schnelle-  
32 Kreis, J., Surratt, J.D., Szidat, S., Szmigielski, R., Wisthaler, A., 2015. The Molecular  
33 Identification of Organic Compounds in the Atmosphere: State of the Art and  
34 Challenges. *Chem. Rev.* 115, 3919–3983. doi:10.1021/cr5003485

- 1 Odian, G.G., 2004. Principles of polymerization. Wiley, Hoboken, N.J.
- 2 Ortiz-Montalvo, D.L., Lim, Y.B., Perri, M.J., Seitzinger, S.P., Turpin, B.J., 2012. Volatility  
3 and Yield of Glycolaldehyde SOA Formed through Aqueous Photochemistry and  
4 Droplet Evaporation. *Aerosol Sci. Technol.* 46, 1002–1014.  
5 doi:10.1080/02786826.2012.686676
- 6 Pearce, S.R.S.K.-A.B.M. (Ed.), 1998. Polymer Synthesis and Characterization. Academic  
7 Press, San Diego.
- 8 Pereira, K.L., Hamilton, J.F., Rickard, A.R., Bloss, W.J., Alam, M.S., Camredon, M., Muñoz,  
9 A., Vázquez, M., Borrás, E., Ródenas, M., 2014. Secondary organic aerosol formation  
10 and composition from the photo-oxidation of methyl chavicol (estragole).  
11 *Atmospheric Chem. Phys.* 14, 5349–5368. doi:10.5194/acp-14-5349-2014
- 12 Pilinis, C., Seinfeld, J.H., Grosjean, D., 1989. Water content of atmospheric aerosols.  
13 *Atmospheric Environ.* 1967 23, 1601–1606. doi:10.1016/0004-6981(89)90419-8
- 14 Renard, P., Reed Harris, A.E., Rapf, R.J., Ravier, S., Demelas, C., Coulomb, B., Quivet, E.,  
15 Vaida, V., Monod, A., 2014. Aqueous Phase Oligomerization of Methyl Vinyl Ketone  
16 by Atmospheric Radical Reactions. *J. Phys. Chem. C* 118, 29421–29430.  
17 doi:10.1021/jp5065598
- 18 Renard, P., Siekmann, F., Gandolfo, A., Socorro, J., Salque, G., Ravier, S., Quivet, E.,  
19 Clément, J.-L., Traikia, M., Delort, A.-M., Voisin, D., Vuitton, V., Thissen, R.,  
20 Monod, A., 2013. Radical mechanisms of methyl vinyl ketone oligomerization  
21 through aqueous phase OH-oxidation: on the paradoxical role of dissolved molecular  
22 oxygen. *Atmospheric Chem. Phys.* 13, 6473–6491. doi:10.5194/acp-13-6473-2013
- 23 Renard, P., Siekmann, F., Salque, G., Demelas, C., Coulomb, B., Vassalo, L., Ravier, S.,  
24 Temime-Roussel, B., Voisin, D., Monod, A., 2015. Aqueous-phase oligomerization of  
25 methyl vinyl ketone through photooxidation – Part 1: Aging processes of oligomers.  
26 *Atmos Chem Phys* 15, 21–35. doi:10.5194/acp-15-21-2015
- 27 Richards-Henderson, N.K., Hansel, A.K., Valsaraj, K.T., Anastasio, C., 2014. Aqueous  
28 oxidation of green leaf volatiles by hydroxyl radical as a source of SOA: Kinetics and  
29 SOA yields. *Atmos. Environ.* 95, 105–112. doi:10.1016/j.atmosenv.2014.06.026
- 30 Rincón, A.G., Calvo, A.I., Dietzel, M., Kalberer, M., 2012. Seasonal differences of urban  
31 organic aerosol composition – an ultra-high resolution mass spectrometry study.  
32 *Environ. Chem.* 9, 298–319.
- 33 Ruuskanen, T.M., Müller, M., Schnitzhofer, R., Karl, T., Graus, M., Bamberger, I., Hörtnagl,  
34 L., Brilli, F., Wohlfahrt, G., Hansel, A., 2011. Eddy covariance VOC emission and

1 deposition fluxes above grassland using PTR-TOF. *Atmospheric Chem. Phys.* 11,  
2 611–625. doi:10.5194/acp-11-611-2011

3 Sempéré, R., Kawamura, K., 2003. Trans-hemispheric contribution of C<sub>2</sub>-C<sub>10</sub> α, ω-  
4 dicarboxylic acids, and related polar compounds to water-soluble organic carbon in  
5 the western Pacific aerosols in relation to photochemical oxidation reactions:  
6 dicarboxylic acids in western pacific aerosols. *Glob. Biogeochem. Cycles* 17, n/a–n/a.  
7 doi:10.1029/2002GB001980

8 Shvartsburg, A.A., Smith, R.D., 2008. Fundamentals of Traveling Wave Ion Mobility  
9 Spectrometry. *Anal. Chem.* 80, 9689–9699. doi:10.1021/ac8016295

10 Smith, J.D., Sio, V., Yu, L., Zhang, Q., Anastasio, C., 2014. Secondary Organic Aerosol  
11 Production from Aqueous Reactions of Atmospheric Phenols with an Organic Triplet  
12 Excited State. *Environ. Sci. Technol.* 48, 1049–1057. doi:10.1021/es4045715

13 Smith, M., March, J., 2007. *March's advanced organic chemistry: reactions, mechanisms, and*  
14 *structure.* Wiley-Interscience, Hoboken, N.J.

15 Spracklen, D.V., Jimenez, J.L., Carslaw, K.S., Worsnop, D.R., Evans, M.J., Mann, G.W.,  
16 Zhang, Q., Canagaratna, M.R., Allan, J., Coe, H., McFiggans, G., Rap, A., Forster, P.,  
17 2011. Aerosol mass spectrometer constraint on the global secondary organic aerosol  
18 budget. *Atmospheric Chem. Phys.* 11, 12109–12136. doi:10.5194/acp-11-12109-2011

19 Tsai, Y., Kuo, S., 2005. PM aerosol water content and chemical composition in a  
20 metropolitan and a coastal area in southern Taiwan. *Atmos. Environ.* 39, 4827–4839.  
21 doi:10.1016/j.atmosenv.2005.04.024

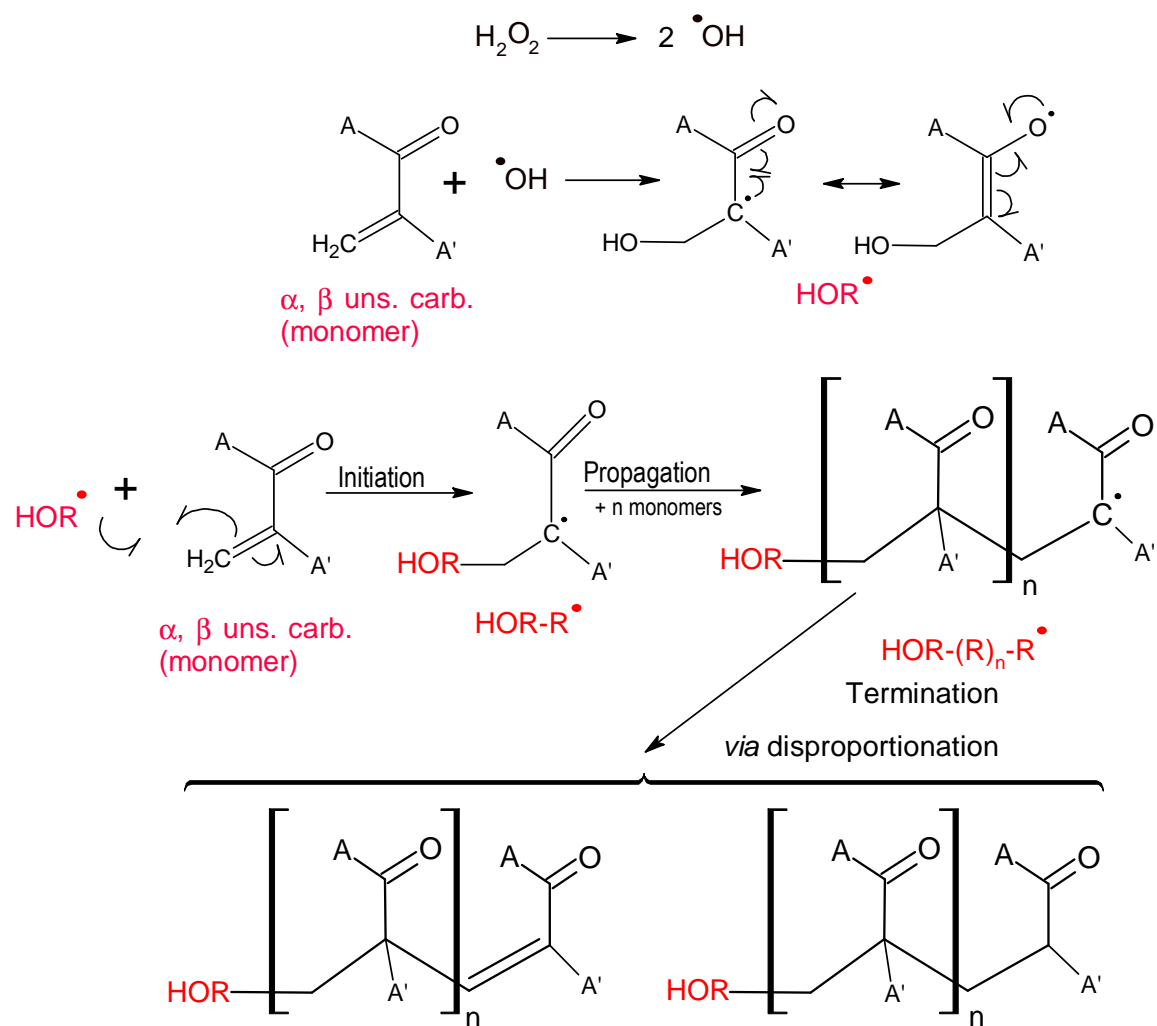
22 Zhao, R., Lee, A.K.Y., Abbatt, J.P.D., 2012. Investigation of Aqueous-Phase Photooxidation  
23 of Glyoxal and Methylglyoxal by Aerosol Chemical Ionization Mass Spectrometry:  
24 Observation of Hydroxyhydroperoxide Formation. *J. Phys. Chem. A* 116, 6253–6263.  
25 doi:10.1021/jp211528d

26  
27  
28  
29  
30  
31  
32  
33  
34  
35  
36



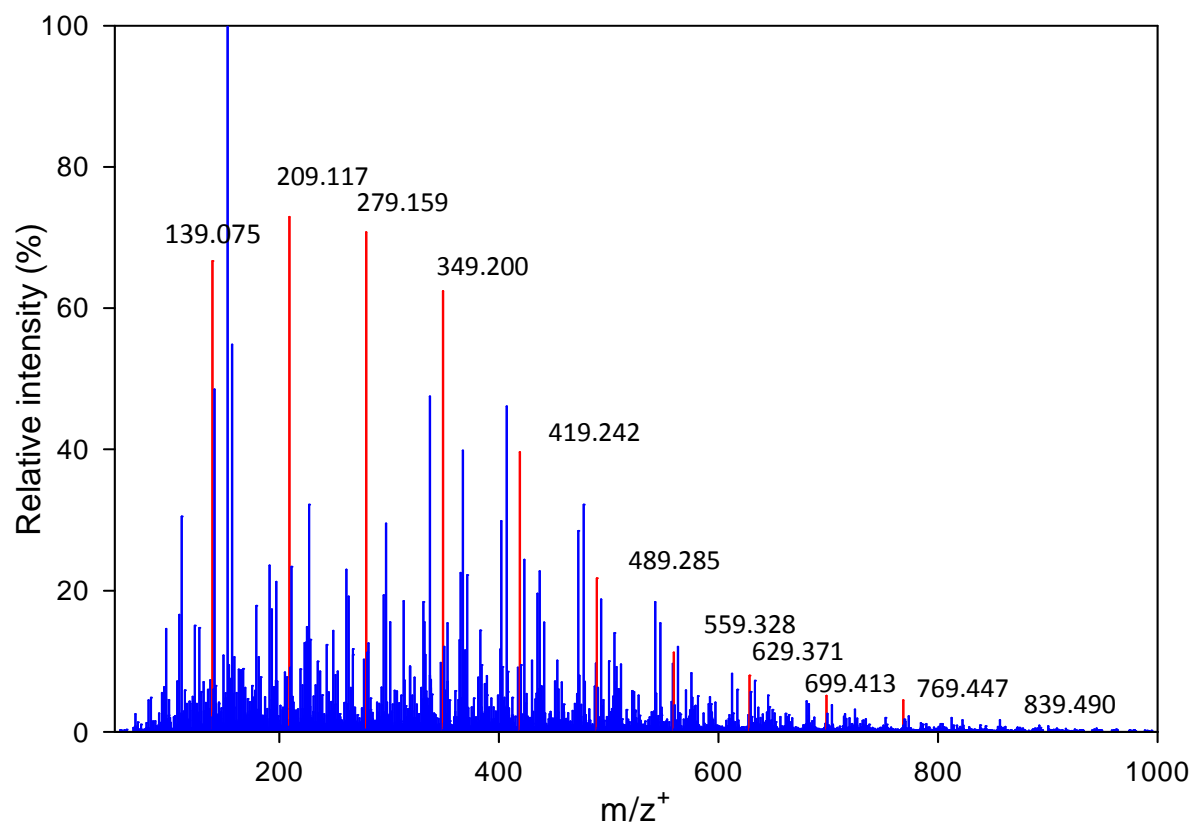
1 **Supplementary information**

2



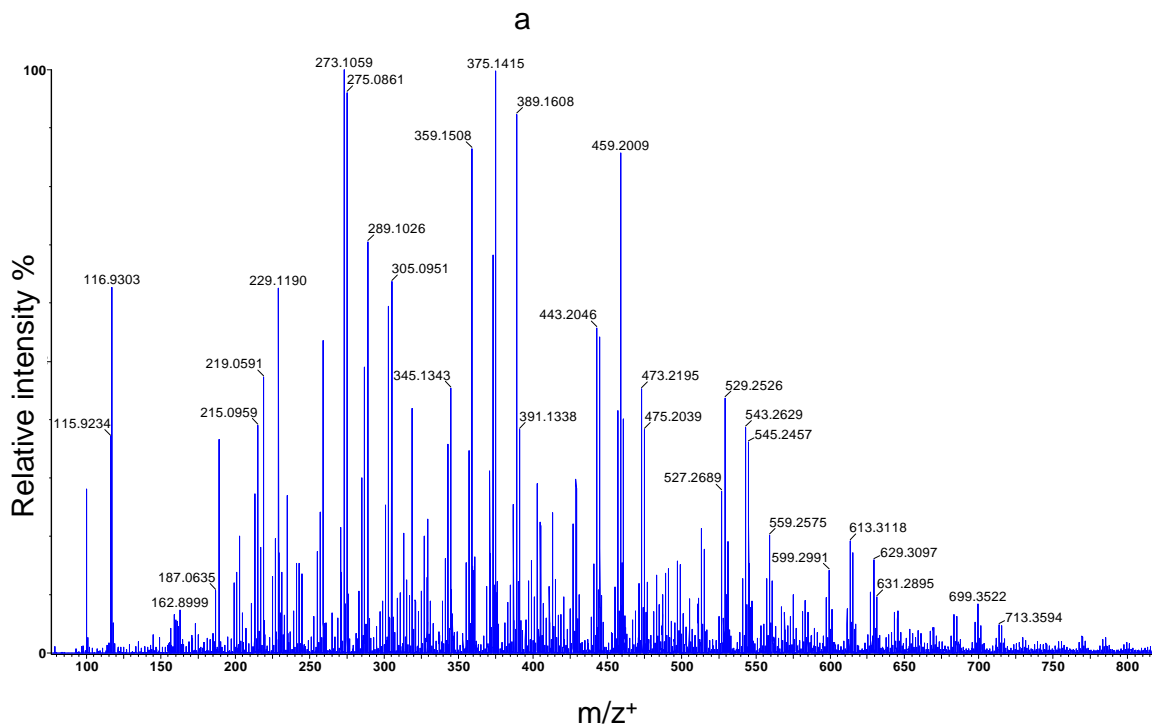
3  
4  
5  
6

**Figure S1:** Vinylic oligomerization of an  $\alpha, \beta$ -unsaturated carbonyl in the aqueous phase, initiated by  $\cdot OH$ -oxidation,  $n$  is the degree of oligomerization i.e. the number of monomers (adapted from Renard et al., 2013).

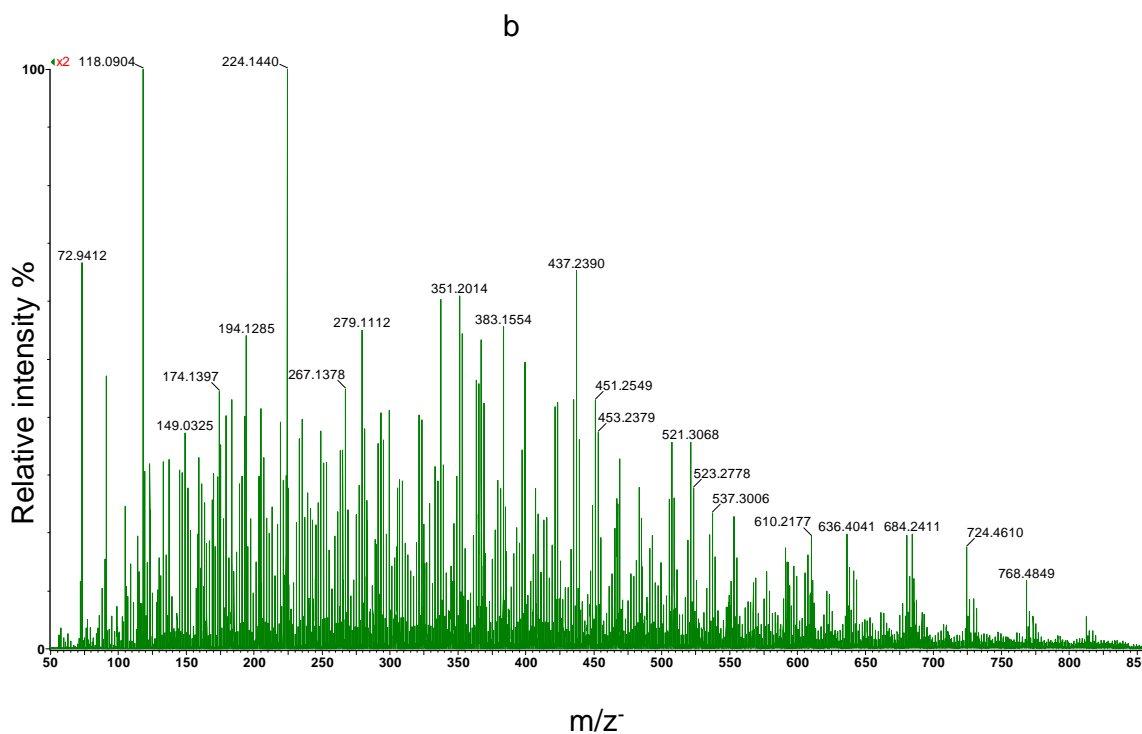


1  
2  
3  
4  
5  
6  
7  
8  
9  
10

**Figure S2:** Typical mass spectrum obtained using UPLC-ESI-MS (in the positive mode) of MVK (20mM) after 50 min of photooxidation in the aqueous phase (highlighted in red, the most intense oligomers series).



1



2  
3  
4  
5  
6

**Figure S3:** Typical mass spectrum obtained using UPLC-ESI-MS of a solution mixture of methyl vinylketone, methacrolein, ethyl vinylketone, methacrylic acid, fumaric and maleic acids (1.67 mM each) after 50 min of photooxidation in the aqueous phase (a) in the positive mode; (b) in the negative mode